

RESEARCH

Open Access



Differences in Fatty Acid Metabolism between MCDD and HFD Induced Metabolic Dysfunction-associated Fatty Liver Disease Model Mice

Jia-Xuan Wang^{1,2}, Xin-Zhu Liu^{3,4}, Zhen Guo^{1,5}, Hui-Lin Zhang¹, Li Qi¹, Jia Liu¹, Ping Liu^{1,3*}, Guo-Xiang Xie^{6,7*} and Xiao-Ning Wang^{1,3*}

Abstract

Background The global incidence of metabolic dysfunction-associated fatty liver disease (MAFLD) is increasing annually, which has become a major public-health concern. MAFLD is typically associated with obesity, hyperlipemia, or metabolic syndrome. Dietary induction is one of the most common methods for preparing animal models of MAFLD. However, there are phenotypic differences between methionine-choline-deficient diet (MCDD) and high fat diet (HFD) models.

Methods To explore the differences in hepatic fatty acid metabolism between MCDD and HFD induced MAFLD, we analyzed serum and liver tissue from the two MAFLD models.

Results We found that liver fat accumulation and liver function damage were common pathological features in both MAFLD models. Furthermore, in the MCDD model, the expression of hepatic fatty acid transport proteins increased, while the expression of hepatic fatty acid efflux proteins and mRNA decreased, along with a decrease in blood lipid levels. In the HFD model, the expression of hepatic fatty acid uptake proteins, efflux proteins and efflux mRNA increased, along with an increase in blood lipid levels.

Conclusion Impaired fatty acid oxidation and increased hepatic fatty acid uptake play key roles in the pathogenesis of the two MAFLD models. The inverse changes in de novo lipogenesis and fatty acid efflux may represent an important pathological mechanism that leads to the phenotypic differences between the MCDD and HFD models.

Keywords Metabolic dysfunction-associated Fatty Liver Disease, Animal Model, Methionine-choline-deficient Diet, High-fat Diet, Fatty Acid Metabolism

*Correspondence:

Ping Liu

liuliver@vip.sina.com

Guo-Xiang Xie

xieguoxiang@hmbiotech.com

Xiao-Ning Wang

wxntcm@126.com

Full list of author information is available at the end of the article



© The Author(s) 2025. **Open Access** This article is licensed under a Creative Commons Attribution-NonCommercial-NoDerivatives 4.0 International License, which permits any non-commercial use, sharing, distribution and reproduction in any medium or format, as long as you give appropriate credit to the original author(s) and the source, provide a link to the Creative Commons licence, and indicate if you modified the licensed material. You do not have permission under this licence to share adapted material derived from this article or parts of it. The images or other third party material in this article are included in the article's Creative Commons licence, unless indicated otherwise in a credit line to the material. If material is not included in the article's Creative Commons licence and your intended use is not permitted by statutory regulation or exceeds the permitted use, you will need to obtain permission directly from the copyright holder. To view a copy of this licence, visit <http://creativecommons.org/licenses/by-nc-nd/4.0/>.

Introduction

Metabolic dysfunction-associated fatty liver disease (MAFLD) is a type of metabolic stress-induced liver damage that is strongly associated with insulin resistance and genetic susceptibility. This condition includes metabolic dysfunction-associated fatty liver, metabolic dysfunction-associated steatohepatitis (MASH), cirrhosis, and hepatocellular carcinoma. The global prevalence of MAFLD among adults is approximately 25% [1]. About 20% MAFLD patients progress to the MASH, which is one of the main causes of cirrhosis and hepatocellular carcinoma [2].

Methods for preparing animal models of MAFLD include dietary induction, gene knockout, and chemical interventions, etc. [3] Dietary induction is convenient and economical, and it includes various types such as methionine-choline-deficient diet (MCDD), high-fat diet (HFD), western diet (WD), high-cholesterol diet (HCD), and choline-deficient L-amino-defined diet (CDAA) [4]. Among these, MCDD and HFD feeding are commonly used to study human MAFLD/MASH; however, there are phenotypic differences between the two MAFLD models. MCDD-fed mice can simulate the process of metabolic dysfunction-associated fatty liver, MASH, and even liver fibrosis [5]. Although most MAFLD patients are accompanied with obesity [6, 7], MCDD feeding for 8 weeks reduced the body weight of mice by about 40% [3, 8–10]. HFD are higher in fat content and HFD-fed mice exhibit obesity, insulin resistance, hepatic steatosis, and liver inflammation, which are similar to the progression characteristics of MAFLD/MASH patients [11, 12]. HFD feeding can simulate the metabolic abnormalities and oxidative stress associated with MAFLD, but it is less effective at progressing to advanced stages such as liver fibrosis [5].

Disruption of fatty acid metabolism can lead to lipid accumulation, obesity, hyperlipidemia, MAFLD, and other related diseases [13]. The liver plays a key role in maintaining systemic carbohydrate and lipid homeostasis [14]. According to previous reports, the *de novo* synthesis, transportation, and oxidation of fatty acids in the liver are important factors for maintaining the fatty acid metabolism homeostasis in the body [4]. To choose suitable and rigorous animal models and develop therapeutic drugs for clinical studies of MAFLD, this study was designed to provide a deeper comparative analysis of the common and specific pathological mechanisms of fatty acid metabolism in MCDD and HFD models.

Materials and methods

Animals and diets

The animal protocol was approved by the Animal Care and Utilization Committee of Shanghai University of Traditional Chinese (authorization code:

PZSHUTCM2212070004). All experiments in this study were performed following the ARRIVE guidelines for reporting experiments involving animals [15]. All methods were carried out in accordance with relevant guidelines and regulations. Male wild-type C57BL/6J mice aged 8 weeks were purchased from Shanghai Xipuer-Beikai Experimental Animal Co, Ltd (license number: SCXK (Shanghai) 2018-0006, lot number: 20180006044350) and maintained in the Experimental Animal Center of Shanghai University of Traditional Chinese Medicine. All mice were housed at 23~24 °C with controlled humidity (60% ± 10%) and with free access to food and drinking water. Mice were fed with MCDD (21-kcal% fat, A02082002BR, Research Diets), or HFD, (42-kcal% fat, TP26300, Nantong TROPHY Feed Technology Co. Ltd), or a standard chow (12.4-kcal% fat, 1010085, Jiangsu Xietong Pharmaceutical Bio-engineering Co., Ltd).

Experimental design

After 1 week of acclimation, the wild-type C57BL/6J mice ($n=32$) were randomly divided into four groups: (1) MCDD-fed control group (MN, $n=8$), (2) MCDD-fed model group (MCDD, $n=8$), (3) HFD-fed control group (HN, $n=8$), and (4) HFD-fed model group (HFD, $n=8$). MCDD group were fed with a MCDD for six weeks [16]. The HFD group were received HFD for twelve weeks [17]. The MN and HN groups were fed with a standard chow for 6 and 12 weeks, respectively (Fig. 1).

Sample collection

At the end of the experiment, all mice in each group were fasted overnight, weighed and then anesthetized with 3% sodium pentobarbital through intraperitoneal injection. Blood samples were collected and centrifugated at 3000 rpm for 20 min at 4 °C and then stored at -80 °C until analysis. The liver tissues were rapidly harvested and weighed. The left liver lobe tissues were freshly collected and fixed in 4% paraformaldehyde for further processing. The other parts of the liver samples were immediately frozen in liquid nitrogen and stored at -80 °C until further analysis.

Biochemical analysis

Serum levels of alanine aminotransferase (ALT), aspartate aminotransferase (AST), alkaline phosphatase (ALP), total cholesterol (TC), triglyceride (TG), high density lipoprotein cholesterol (HDL-C), low density lipoprotein cholesterol (LDL-C) were determined at Center for Drug Safety Evaluation and Research, Shanghai University of Traditional Chinese Medicine according to the manufacturer's instructions of the commercial kits determined on an automatic biochemical analyzer (TBA-40FR, TOSHIBA, Japan).

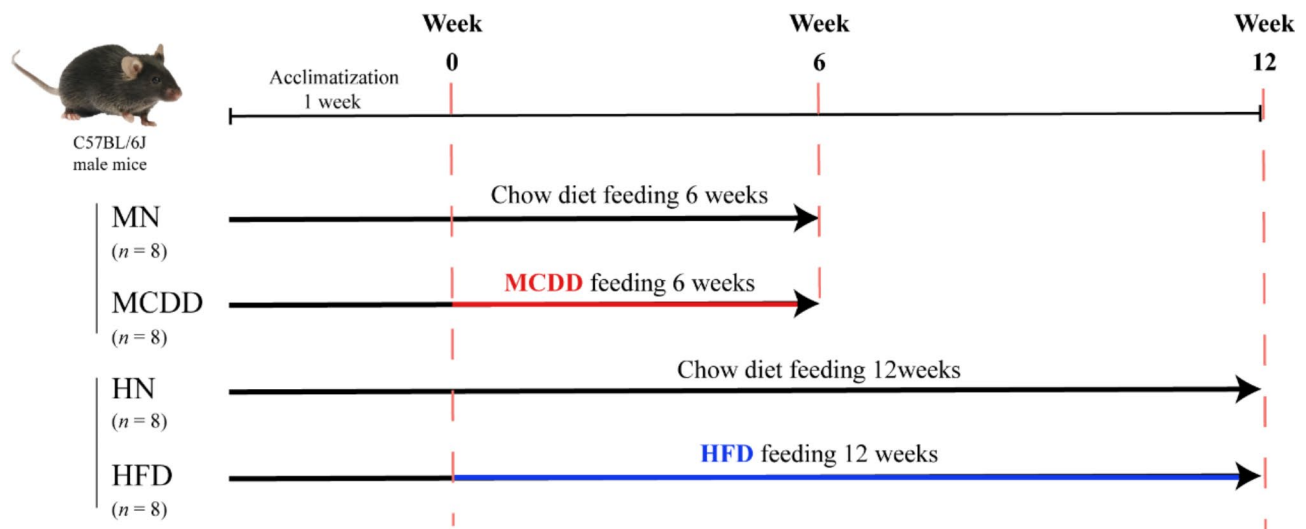


Fig. 1 Scheme of the experiment

Hepatic free fatty acids (FFA) and TG were measured according to the instructions of the manufacturer of commercial kits (Nanjing Jiancheng Bioengineering Institute, Nanjing, China).

Histopathological evaluation

The liver tissue samples were immersed in 4% paraformaldehyde to achieve adequate fixation, dried, and embedded in paraffin to produce paraffin slices. Hematoxylin and eosin (H&E) and Oil Red O were used to stain the slices, and a light microscope was used to examine and take pictures of the pathological characteristics of the liver tissue. Image J software was used to semi-quantitatively measure positively stained area of Oil Red O staining. Histological features of the liver were evaluated according to the Kleiner scoring system as previously described [18], and the sum of these pathological features was used to estimate the MAFLD activity score (NAS).

RNA isolation and quantitative RT-PCR

Total liver RNA was isolated by the TRIzol reagent and used for cDNA synthesis based on the manufacturer's protocol (BioTNT, China). Then qRT-PCR was operated using a CFX Connect Real-time PCR system (BIO-RAD, USA). The level of the internal reference (β -actin) gene was used as the internal control for normalization of the results, and each mRNA expression was calculated via the $2^{-\Delta\Delta C_t}$ method [19]. The following primers of target genes (purchased from BioTNT, China): mouse Fas alpha Forward CCC GCT GTT TTC CCT TGC T, mouse Fas beta Forward ATC AGT TTC ACG AAC CCG CCT; mouse ApoB100 alpha Forward TGC TCA CAA GGC AAC ACT AAA, mouse ApoB100 beta Forward GCA TTC AAC TCA TTC TCC AGC; mouse MTTP alpha Forward CCA CCA GAA TCG TAA GGT TCA, mouse

MTTP beta Forward GGA CAG CAG GAT GTT CTT CAC; mouse β -actin alpha Forward CCT CTA TGC CAA CAC AGT, mouse β -actin beta Forward AGC CAC CAA TCC ACA CAG.

Western blot analysis

Fast-frozen liver tissues were weighed, completely homogenized, and lysed. Equal amounts of protein determined using BCA kits were separated on 10% SDS-PAGE; transferred onto PVDF membranes; blocked with 5% BSA; and incubated with the diluted primary antibodies sterol regulatory element binding proteins (SREBP-1c, sc-13551, Santa Cruz, USA), fatty acid synthase (FAS, C20G5, CST, USA), peroxisome proliferators activated receptor α (PPAR α , ab215270, Abcam, UK), acyl-coenzyme A oxidase 1 (ACOX1, ab184032, Abcam, UK), recombinant apolipoprotein B100 (ApoB100, ab20737, Abcam, UK), recombinant microsomal triglyceride transfer protein (MTTP, ab75316, Abcam, UK), carnitine palmitoyl transferase-1 α (CPT1 α , ab128568, Abcam, UK), fatty acid translocase CD36 (CD36, ab124515, Abcam, UK), acetyl CoA carboxylase 1 (ACC1, 21923-1-AP, Proteintech, USA), glyceraldehyde 3-phosphate dehydrogenase (GAPDH, 60004-1-Ig, Proteintech, USA), fatty acid transport protein 2 (FATP2, 14048-1-AP, Proteintech, USA) overnight at 4°C. Afterwards, the membrane was washed with TBST and incubated with a secondary antibody (Beyotime Institute of Biotechnology, China). The blotted protein bands were detected by chemiluminescent assay kit, and the protein expression levels were normalized to GAPDH (Proteintech) by densitometry using the ImageJ software (<http://rsb.info.nih.gov/ij/>; National Institutes of Health, Bethesda, MD, USA).

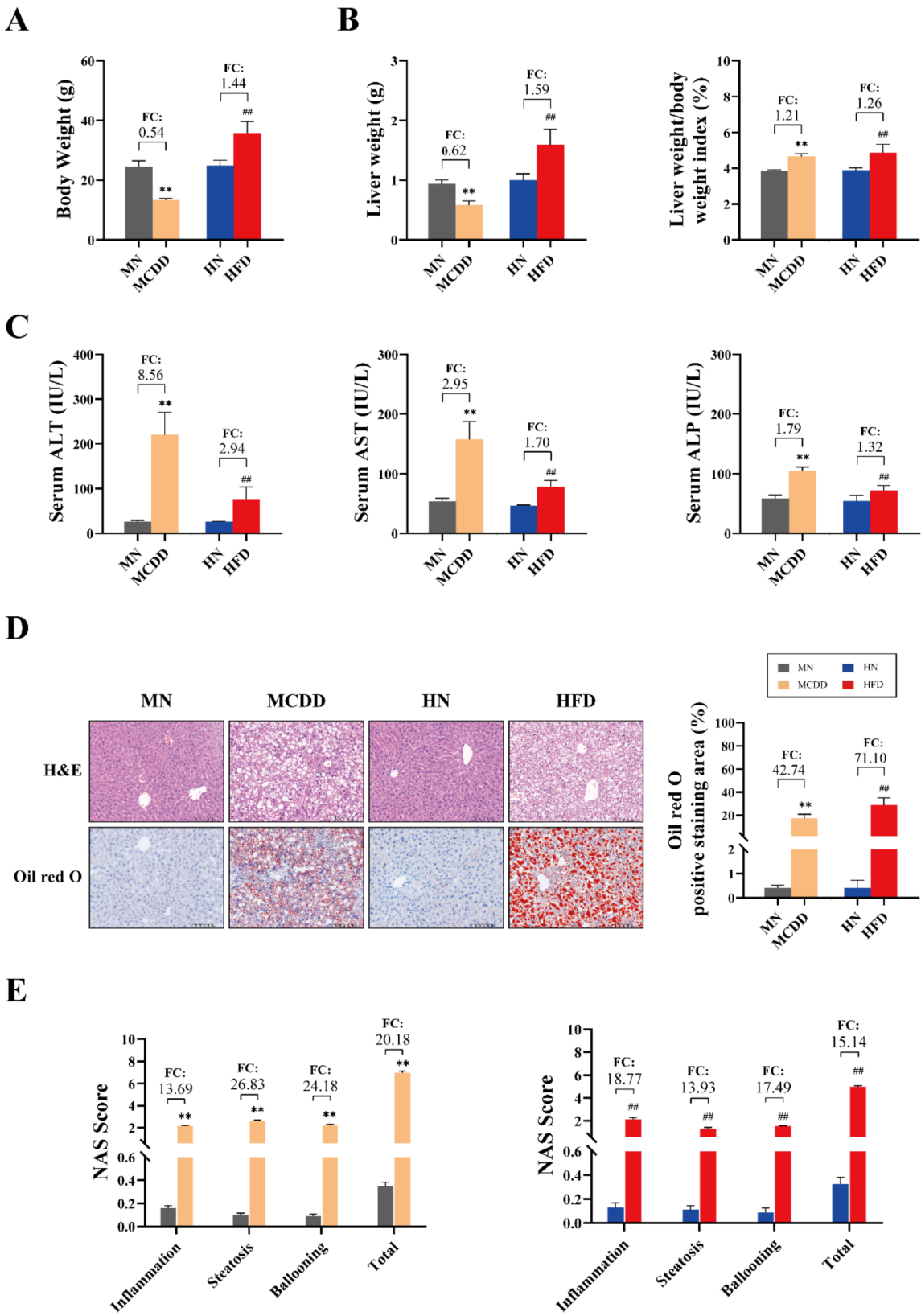


Fig. 2 (See legend on next page.)

(See figure on previous page.)

Fig. 2 Liver function and liver histopathological changes of mice in each group. **(A)** Body weight. **(B)** Liver weight and the liver weight to body weight ratio of the experimental mice at the end of study. **(C)** Serum levels of ALT, AST and ALP. **(D)** H&E (left up panel) and Oil Red O (left down panel) staining for hepatic sections representative images of quantification of liver steatosis by assessing the Oil Red O area ratio (right panel) 200 \times , 100 μ m. **(E)** NAS scores. Data were expressed as the means \pm SD. * $P < 0.05$, ** $P < 0.01$ vs. MN group. # $P < 0.05$, ## $P < 0.01$ vs. HN group. FC, fold change, model-to-normal group ratio. MN, standard chow diet; MCDD, methionine-choline-deficient diet; HN, standard chow diet; HFD, high-fat diet

Statistical analysis

All Statistical analyses were performed using SPSS software (Version 27.0, IBM, Armonk, NY, USA) and Graph-Pad Prism (Version 8.0, San Diego, California, USA). Data were evaluated by Unpaired t test and expressed as mean \pm standard deviation (SD). Statistical significance was defined as $P < 0.05$.

Results

Liver fat accumulation and liver function damage in MCDD and HFD models

Wild-type C57BL/6J male mice were fed MCDD for 6 weeks and HFD for 12 weeks to induce MAFLD. Compared with the MCDD-fed control group (MN) group, the body weight and liver weight of mice in the MCDD group were significantly reduced, while the liver to body weight ratio was significantly increased ($P < 0.01$). In comparison to the HFD-fed control group (HN) group, the body weight, liver weight and liver to body weight ratio of mice in the HFD group were significantly increased ($P < 0.01$) (Fig. 2A-B). Serum ALT, AST, and ALP activities were significantly increased in both the MCDD group and HFD group ($P < 0.01$) (Fig. 2C).

Histological analysis using H&E and Oil Red O staining of the liver tissue showed that the structure of liver lobules in the MN group and HN group was intact, with liver cords neatly arranged. In contrast, the MCDD group exhibited large vacuolar steatosis in the central vein area and inflammatory infiltrates in the liver lobules. The HFD group displayed a mixed pattern of large and small vacuolar steatosis, along with diffuse inflammation and significant fat accumulation. Oil Red O staining also demonstrated that the positive staining area, liver inflammation, steatosis, ballooning, and total NAS scores were significantly increased in both the MCDD group and the HFD group compared to their respective control group ($P < 0.01$) (Fig. 2D-E).

Impaired fatty acid oxidation in MCDD and HFD models

Fatty acid oxidation is an important way for metabolizing fatty acids and producing ATP. Key proteins involved in fatty acid oxidation include PPAR α , carnitine palmitoyltransferase 1 α (CPT1 α), and ACOX1. Western blot analysis revealed that the protein expressions of PPAR α , CPT1 α , and ACOX1 in the liver tissues of both the MCDD group and the HFD group were significantly lower than those in the respective normal control groups

($P < 0.01$) (Fig. 3A-B). These findings suggested that fatty acid oxidation was impaired in both MAFLD models.

Fatty acid metabolism in MCDD and HFD models

Biochemical analysis indicated significant decreases in serum total cholesterol (TC), triglycerides (TG), high-density lipoprotein cholesterol (HDL-C), and low-density lipoprotein cholesterol (LDL-C) levels in the MCDD group compared to the MN group. In contrast, the HFD group exhibited significant increases in these parameters compared to the HN group (Fig. 4A). Both the MCDD and HFD groups exhibited significant increases in hepatic free fatty acid (FFA) and TG levels compared to their respective control groups, with a more pronounced effect observed in the HFD group (Fig. 4B).

Western blot analysis showed that the expressions of CD36 and FATP2 in the liver tissue of both the MCDD and HFD groups were significantly increased compared to their respective control groups ($P < 0.01$) (Fig. 4C). Additionally, compared to the MN group and the HN group, respectively, the expressions of ApoB100 and microsomal triglyceride transfer protein (MTTP) proteins in the liver tissue of the MCDD group were decreased, while the expressions were increased in the HFD group ($P < 0.01$) (Fig. 4D). Consistently, the mRNA expressions of ApoB100 and MTTP were decreased in the MCDD group when compared to the MN group ($P < 0.05$, $P < 0.01$), while the mRNA expressions of ApoB100 and MTTP in the HFD group were increased compared to the HN group ($P < 0.05$) (Fig. 4E-F).

De novo lipogenesis is reduced in MCDD group and increased in the HFD group

De novo lipogenesis in liver cells is an important source of fatty acids in the body. SREBP-1c, FAS, and ACC1 are key factors in regulating de novo lipogenesis. Compared to the MN group, the protein expressions of SREBP-1c, FAS, and ACC1, as well as the mRNA expression of FAS in liver tissue of the MCDD group, were significantly reduced ($P < 0.01$) (Fig. 5A-C). In contrast, compared to the HN group, the expressions of SREBP-1c, FAS, ACC1 and the mRNA expression of FAS in the HFD group was significantly increased ($P < 0.05$, $P < 0.01$) (Fig. 5A-C).

Discussion

Consistent with previous reports on MCDD and HFD-induced MAFLD [20–26], mice developed mild inflammation and liver fat accumulation within 2 weeks of

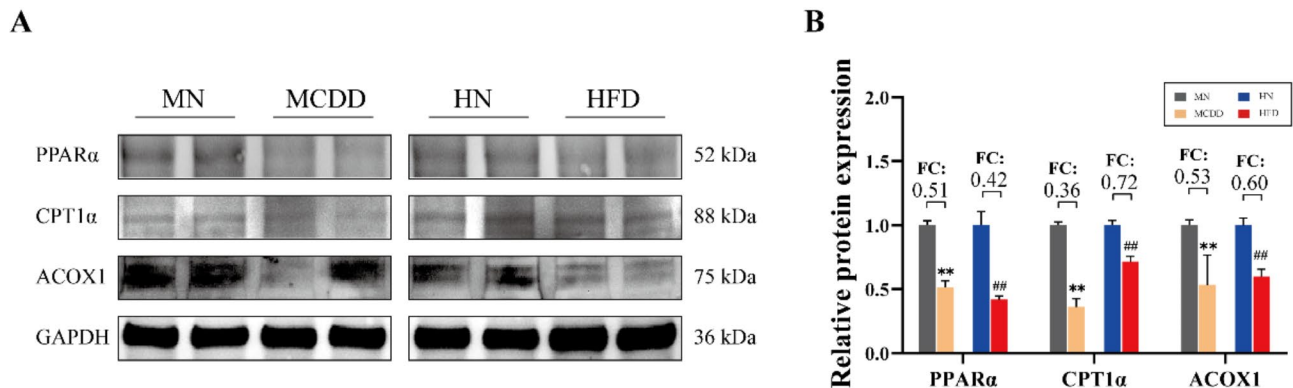


Fig. 3 Changes in expression of fatty acid oxidation-related proteins in mice in each group. **(A-B)** Western blot results for PPARα, CPT1α and ACOX1 in liver samples. Data were expressed as the means ± SD. * $P < 0.05$, ** $P < 0.01$ vs. MN group. # $P < 0.05$, ## $P < 0.01$ vs. HN group. FC, fold change, model-to-normal group ratio. MN, standard chow diet; MCDD, methionine-choline-deficient diet; HN, standard chow diet; HFD, high-fat diet

intervention, followed by severe inflammation and fibrosis of liver tissue after 4 to 6 weeks of intervention. Methionine is an essential amino acid for the human body, playing a pivotal role in physiological processes such as maintaining cellular redox homeostasis [27]. A deficiency in methionine can result in impaired production of various metabolites, which may lead to rapid weight loss in animals [28, 29]. The body weight and liver weight of MCDD-fed mice were decreased, while those of HFD-fed mice were increased [30–32]. Lipotoxicity is one of the main causes of liver cell dysfunction in MAFLD [20]. HE staining and Oil Red O staining of the liver confirmed that significant steatosis was observed in both the MCDD and HFD groups. Serum ALT, AST, and ALP results indicated liver function impairment in both the MCDD and HFD groups, with greater liver damage observed in the MCDD group.

Fatty acid oxidation is an important pathway of fatty acid metabolism, including mitochondrial β -oxidation, peroxisomal β -oxidation, and microsomal ω -oxidation [21]. PPARα is a widely expressed nuclear transcription factor in the liver that is closely associated with fatty acid oxidation and transport [33]. PPARα activates downstream proteins such as CPT1α and ACOX1, synergistically promoting lipid and lipoprotein metabolism while inhibiting obesity and liver fat accumulation [13, 34]. The carnitine shuttle facilitates the import of long-chain fatty acid into the mitochondria, as the mitochondrial inner membrane is impermeable to them. This system includes CPT1, acylcarnitine translocase (CACT), and CPT2 [35]. CPT1α is localized in the outer mitochondrial membrane, where it transports long-chain acylcarnitines into the mitochondrial matrix, and then CPT2 converts long-chain acylcarnitines back to long-chain acyl-CoAs [36, 37]. CPT1α is closely involved in mitochondrial oxidation and is a key factor that regulates the entry of fatty acids into the mitochondrial matrix. A decreased expression of CPT1α promotes liver damage and fat

accumulation [38]. ACOX1 is involved in the first step of peroxisomal β -oxidation and is the rate-limiting enzyme of the peroxisomal fatty acid oxidation system, preferentially metabolizes straight-chain fatty acids [39]. Both the MCDD and HFD groups had significantly lower protein expression of PPARα, CPT1α, and ACOX1 in liver tissue compared to the control group, suggesting that hepatic fatty acid oxidation capacity was impaired in two of MAFLD mice.

Methionine is a component of antioxidants, and choline is related to the synthesis of phosphatidylcholine [40]. Methionine and choline are key factors in mitochondrial oxidation and the synthesis of very-low-density lipoproteins (VLDL) in the liver. Antioxidants help inhibit oxidative stress and improve metabolic homeostasis [41]. A deficiency of both will lead to impaired fatty acid metabolism and TG transport in the liver, resulting in increased liver TG accumulation [42, 43]. Significantly decreased serum TC, TG, HDL-C, and LDL-C levels, along with significantly increased liver FFA and TG levels observed in MCDD mice were consistent with previous literature findings [43].

HFD feeding causes adipocyte hypertrophy and expansion of adipose tissue [44]. Excessive intake of fatty acids and carbohydrates due to HFD leads to calorie overload and upregulation of proteins involved in fatty acid uptake, de novo synthesis, and lipid droplet formation in the liver, resulting in increased TG synthesis [45, 46]. This study found significant increases in serum TC, TG, HDL-C, LDL-C levels, as well as increased liver FFA and TG contents in the HFD group, accompanied by significant liver fat accumulation.

The proper functionality of hepatic fatty acid uptake and efflux is closely related to the pathogenesis of MAFLD. Free fatty acids produced by adipose tissue lipolysis enter the liver through the bloodstream, contributing to liver fat accumulation [7]. CD36, located on the cell membrane, acts as a fatty acid transferase to

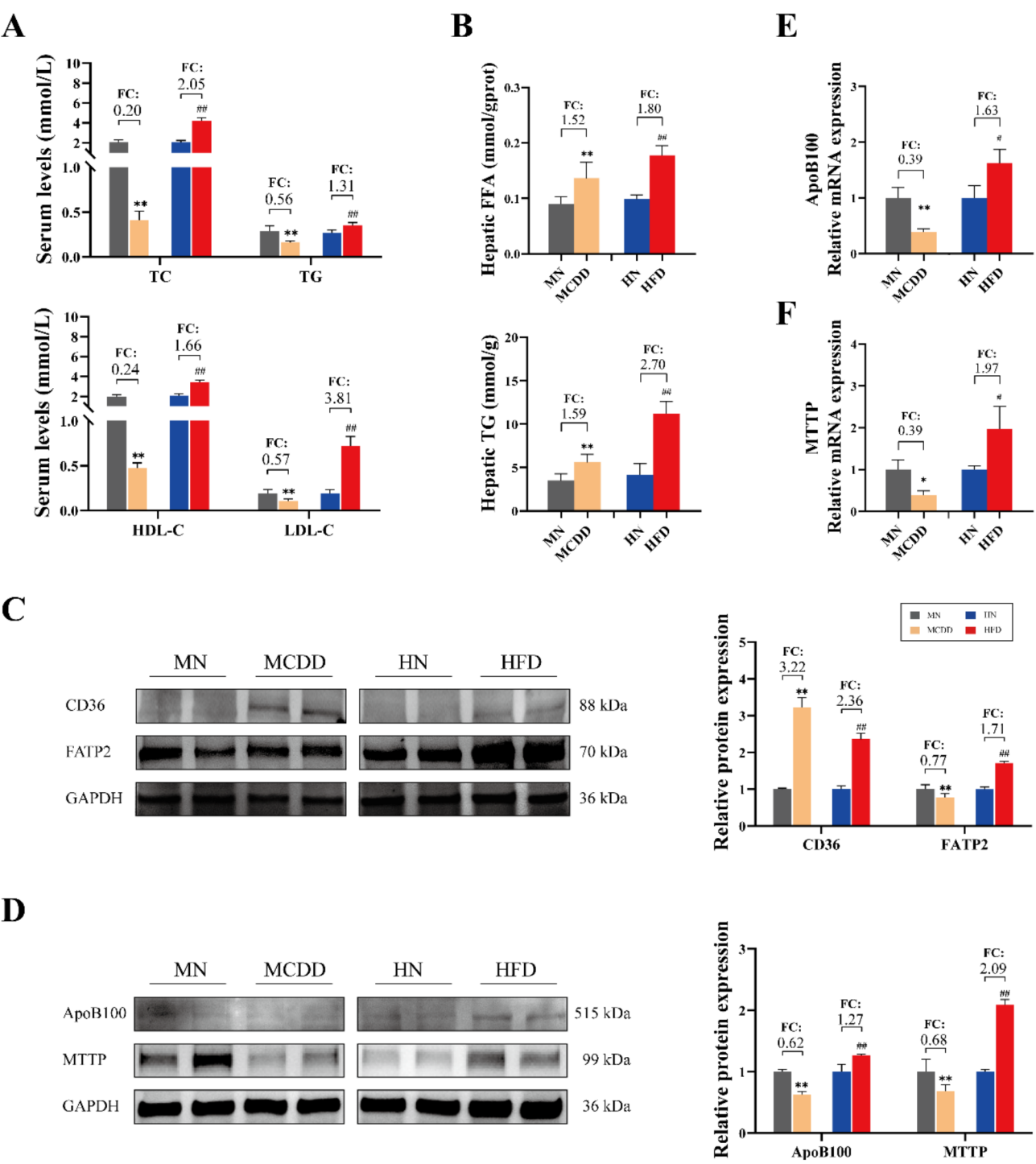


Fig. 4 Blood lipids, hepatic FFA and TG contents, the protein and mRNA expression of liver tissues. **(A)** Serum TC, TG, HDL-C and LDL-C levels were assessed. **(B)** Hepatic FFA, TG levels were assessed. **(C)** Western blot results for CD36, FATP2 in liver samples. **(D)** Western blot results for ApoB100, MTTP in liver samples. **(E-F)** ApoB100 and MTTP gene levels of liver samples were measured through qRT-PCR, and normalized against β -actin level. Data were expressed as the means \pm SD. * $P < 0.05$, ** $P < 0.01$ vs. MN group. # $P < 0.05$, ## $P < 0.01$ vs. HN group. FC, fold change, model-to-normal group ratio. MN, standard chow diet; MCDD, methionine-choline-deficient diet; HN, standard chow diet; HFD, high-fat diet

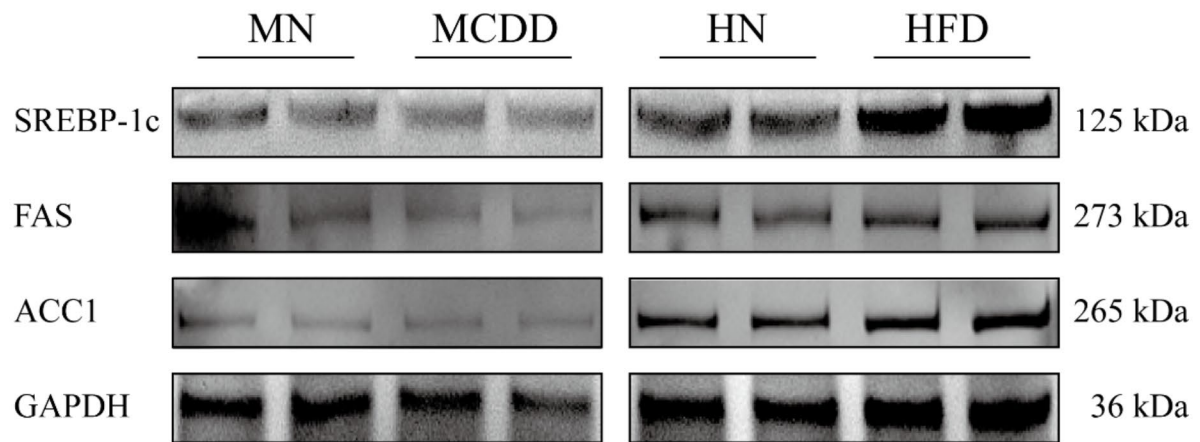
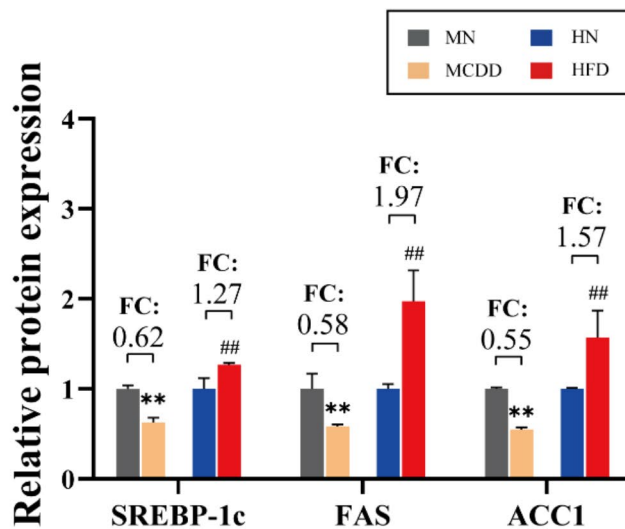
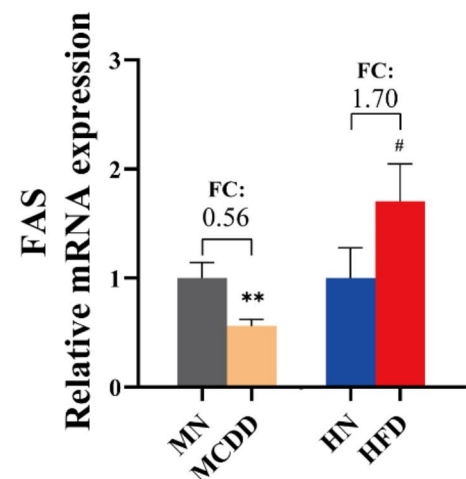
A**B****C**

Fig. 5 The expression of proteins and mRNA in the liver of mice in each group. **(A-B)** Western blot results for FAS, ACC1, SREBP-1c in liver samples. **(C)** FAS gene levels of liver samples were measured through qRT-PCR, and normalized against β -actin level. Data were expressed as the means \pm SD. * P <0.05, ** P <0.01 vs. MN group. # P <0.05, ## P <0.01 vs. HN group. FC, fold change, model-to-normal group ratio. MN, standard chow diet; MCDD, methionine-choline-deficient diet; HN, standard chow diet; HFD, high-fat diet

transport free fatty acids from outside the liver into hepatocytes together with FATP2. Increased CD36 expression promotes fat accumulation in liver cells. CD36 is involved not only the uptake of free fatty acids, but also regulates SREBP1 proteolysis [47]. HFD-fed results in a higher cellular input of fatty acids and less fatty acid output via oxidation or export, resulting in fat accumulation in hepatocytes [48]. Consistent with these findings, this study also observed significant increases in the expression of CD36 and FATP2 proteins in the liver tissue of mice in MCDD and HFD group, indicating increased fatty acid uptake and decreased, accelerating the flow of

free fatty acids from the extrahepatic to the intrahepatic, and thus leading to the accumulation of liver fat.

The size of the liver FFA pool is related to VLDL-TG and de novo fatty acid synthesis [49]. VLDL is an important carrier for transporting liver TG to the peripheral blood. ApoB100 is the main structural component of VLDL, and decreased ApoB100 expression inhibits the transfer of liver TG to the periphery. MTTP is an endoplasmic reticulum lipid transfer protein that plays a key role in lipoprotein assembly, assisting ApoB100 in the lipidation of nascent VLDL and the transfer of neutral lipids between vesicles [50]. This study found decreased expression of ApoB100 and MTTP mRNA and proteins

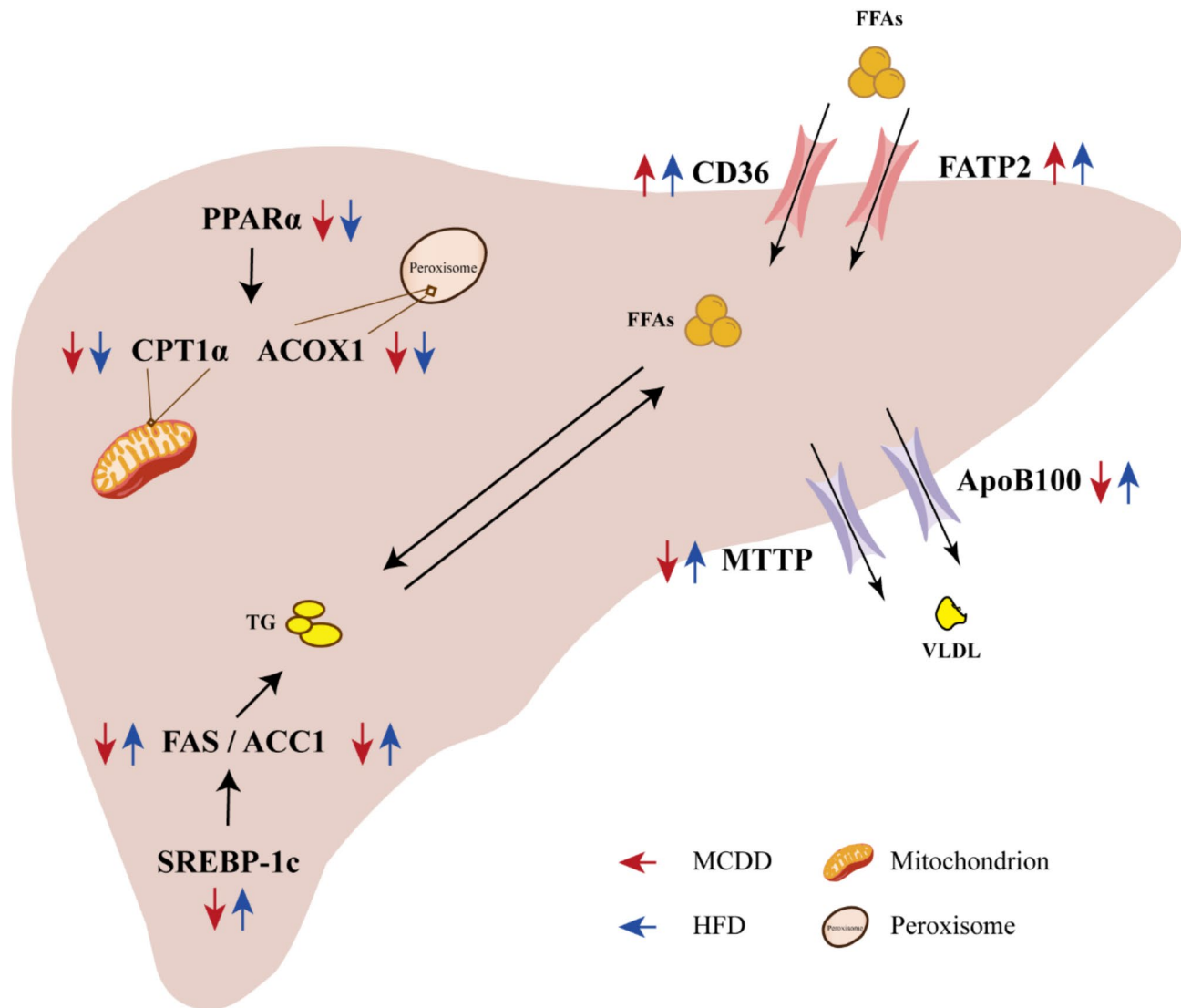


Fig. 6 Differences in fatty acid de novo synthesis and outward hepatic transport between two models

in the liver tissue of the MCDD group, leading to reduced TG efflux from the liver, increased liver lipid accumulation, decreased peripheral blood lipid levels, and severe malnutrition. The HFD group showed increased expression of ApoB100 and MTTP mRNA and proteins, leading to increased TG efflux, leading to a significant increase in circulating blood lipid levels.

The elevated de novo synthesis of fatty acids is a crucial step in the accumulation of TG in hepatocytes. Activated SREBP-1c translocates to the nucleus and upregulates the expression of downstream FAS and ACC1, promoting fatty acid synthesis [51]. The process of MCDD-induced hepatic fat accumulation differs from the HFD-induced mechanisms and is not directly linked to de novo lipogenesis [52]. We found that the expressions of FAS mRNA and the proteins SREBP-1c, FAS, ACC1 in the liver tissue of MCDD group mice were lower than that of the MN

group, whereas the expression of FAS mRNA and these three proteins in the liver tissue of HFD group mice were higher than that of the HN group. De novo lipogenesis was reduced in MCDD group mice but increased in HFD group mice, which may represent the specific pathological mechanism for the phenotypic differences between the two MAFLD mouse models. Increased de novo lipogenesis may be one of the important reasons for fat accumulation in liver tissue and increased blood lipid levels in HFD group mice.

Conclusions

In summary, MCDD feeding can induce severe MASH-related fibrosis in a short period, while HFD feeding can induce mild liver injury that is similar to that observed in the majority of MAFLD patients, albeit with a slower progression over time. Hepatic fat accumulation and liver

function impairment are common pathological features of in both MAFLD diets. Impaired fatty acid oxidation, and increased fatty acid uptake are shared pathological mechanisms across both forms of MAFLD. The inverse changes in de novo lipogenesis and fatty acid efflux may represent an important pathological mechanism leading to the phenotypic differences between MCDD-fed and HFD-fed mice (Fig. 6).

Acknowledgements

Not applicable.

Author Contributions

X.N.W., G.X.X. and P.L. designed this study. J.X.W. performed all experiments. X.Z.L. drafted the manuscript. Z.G. performed data analysis. H.L.Z., L.Q., and J.L. assisted in collecting the samples. All authors critically revised the manuscript and approved the final manuscript.

Funding

This research was funded by the National Natural Science Foundation of China (81774196) and the Natural Science Foundation of Shanghai Municipality of China (22ZR1459200).

Data Availability

No datasets were generated or analysed during the current study.

Declarations

Ethics Approval and Consent to Participate

The animal protocol was approved by the Animal Care and Utilization Committee of Shanghai University of Traditional Chinese (authorization code: PZSHUTCM2212070004).

Consent for Publication

Not applicable.

Competing Interests

The authors declare no competing interests.

Author details

¹Institute of Interdisciplinary Science, Shanghai University of Traditional Chinese Medicine, Shanghai 201203, China

²Department of Hepatology, Yueyang Hospital of Integrated Traditional Chinese and Western Medicine, Shanghai University of Traditional Chinese Medicine, Shanghai 200437, China

³Institute of Liver Disease, Shuguang Hospital, Shanghai University of Traditional Chinese Medicine, Shanghai 201203, China

⁴Shanghai Municipal Hospital of Traditional Chinese Medicine, Shanghai University of Traditional Chinese Medicine, Shanghai 200071, China

⁵The Affiliated Traditional Chinese Medicine Hospital, Southwest Medical University, Sichuan 646000, China

⁶Human Metabolomics Institute, Inc., Shenzhen 518109, Guangdong, China

⁷Faculty of Food Science and Engineering, Kunming University of Science and Technology, Kunming 650500, China

Received: 4 February 2025 / Accepted: 28 March 2025

Published online: 14 April 2025

References

- Huang DQ, El-Serag HB, Loomba R. Global epidemiology of NAFLD-related HCC: trends, predictions, risk factors and prevention. *Nat Rev Gastroenterol Hepatol*. 2021;18(4):223–38.
- Lazarus JV, Mark HE, Villota-Rivas M, Palayew A, Carrieri P, Colombo M, Ekstedt M, Esmat G, George J, Marchesini G, et al. The global NAFLD policy review and preparedness index: are countries ready to address this silent public health challenge? *J Hepatol*. 2022;76(4):771–80.
- Wang H, Shen H, Seo W, Hwang S. Experimental models of fatty liver diseases: status and appraisal. *Hepatol Commun*. 2023;7(7):e200.
- Yu Y, Cai J, She Z, Li H. Insights into the epidemiology, pathogenesis, and therapeutics of nonalcoholic fatty liver diseases. *Adv Sci (Weinh)*. 2019;6(4):1801585.
- Alshawh MA, Alsalahi A, Alshehade SA, Saghir SAM, Ahmeda AF, Al Zarzour RH, Mahmoud AM. A comparison of the gene expression profiles of Non-Alcoholic fatty liver disease between animal models of a High-Fat diet and Methionine-Choline-Deficient diet. *Molecules*. 2022;27(3):858.
- Younossi ZM, Koenig AB, Abdelatif D, Fazel Y, Henry L, Wymer M. Global epidemiology of nonalcoholic fatty liver disease—Meta-analytic assessment of prevalence, incidence, and outcomes. *Hepatology*. 2016;64(1):73–84.
- Willis SA, Bawden SJ, Malaikah S, Sargeant JA, Stensel DJ, Aithal GP, King JA. The role of hepatic lipid composition in obesity-related metabolic disease. *Liver Int*. 2021;41(12):2819–35.
- Xu R, Pan J, Zhou W, Ji G, Dang Y. Recent advances in lean NAFLD. *Biomed Pharmacother*. 2022;153:113331.
- Machado MV, Michelotti GA, Xie G, Almeida Pereira T, Boursier J, Bohnic B, Guy CD, Diehl AM. Mouse models of diet-induced nonalcoholic steatohepatitis reproduce the heterogeneity of the human disease. *PLoS ONE*. 2015;10(5):e0127991.
- Friedman SL, Neuschwander-Tetri BA, Rinella M, Sanyal AJ. Mechanisms of NAFLD development and therapeutic strategies. *Nat Med*. 2018;24(7):908–22.
- Nezvorova YA, Boyer-Diaz Z, Cubero FJ, Gracia-Sancho J. Animal models for liver disease - A practical approach for translational research. *J Hepatol*. 2020;73(2):423–40.
- Fang T, Wang H, Pan X, Little PJ, Xu S, Weng J. Mouse models of nonalcoholic fatty liver disease (NAFLD): pathomechanisms and pharmacotherapies. *Int J Biol Sci*. 2022;18(15):5681–97.
- Lee H, Ahn J, Shin SS, Yoon M. Ascorbic acid inhibits visceral obesity and nonalcoholic fatty liver disease by activating peroxisome proliferator-activated receptor α in high-fat-diet-fed C57BL/6J mice. *Int J Obes (Lond)*. 2019;43(8):1620–30.
- Honma M, Sawada S, Ueno Y, Murakami K, Yamada T, Gao J, Kodama S, Izumi T, Takahashi K, Tsukita S, et al. Selective insulin resistance with differential expressions of IRS-1 and IRS-2 in human NAFLD livers. *Int J Obes (Lond)*. 2018;42(9):1544–55.
- McGrath JC, Lilley E. Implementing guidelines on reporting research using animals (ARRIVE etc): new requirements for publication in *BJP. Br J Pharmacol*. 2015;172(13):3189–93.
- Liu Y, Xu W, Zhai T, You J, Chen Y. Silibinin ameliorates hepatic lipid accumulation and oxidative stress in mice with non-alcoholic steatohepatitis by regulating CFLAR-JNK pathway. *Acta Pharm Sin B*. 2019;9(4):745–57.
- Xu W, Cui C, Cui C, Chen Z, Zhang H, Cui Q, Xu G, Fan J, Han Y, Tang L, et al. Hepatocellular cystathionine γ lyase/hydrogen sulfide attenuates nonalcoholic fatty liver disease by activating farnesoid X receptor. *Hepatology*. 2022;76(6):1794–810.
- León-Mimila P, Villamil-Ramírez H, Li XS, Shih DM, Hui ST, Ocampo-Medina E, López-Contreras B, Morán-Ramos S, Olivares-Arevalo M, Grandini-Rosales P, et al. Trimethylamine N-oxide levels are associated with NASH in obese subjects with type 2 diabetes. *Diabetes Metab*. 2021;47(2):101183.
- Akoumi A, Haffar T, Moustherji M, Kiss RS, Boussette N. Palmitate mediated Diacylglycerol accumulation causes Endoplasmic reticulum stress, Plin2 degradation, and cell death in H9C2 cardiomyoblasts. *Exp Cell Res*. 2017;354(2):85–94.
- Sanhueza S, Tobar N, Cifuentes M, Quenti D, Vari R, Scazzocchio B, Masella R, Herrera K, Paredes A, Morales G, et al. Lampaya medicinalis phil. Decreases lipid-induced triglyceride accumulation and Proinflammatory markers in human hepatocytes and fat body of drosophila melanogaster. *Int J Obes (Lond)*. 2021;45(7):1464–75.
- Geng Y, Faber KN, de Meijer VE, Blokzijl H, Moshage H. How does hepatic lipid accumulation lead to lipotoxicity in non-alcoholic fatty liver disease? *Hepatol Int*. 2021;15(1):21–35.
- Yabiku K, Nakamoto K, Tsubakimoto M. Effects of Sodium-Glucose Cotransporter 2 Inhibition on Glucose Metabolism, Liver Function, Ascites, and Hemodynamics in a Mouse Model of Nonalcoholic Steatohepatitis and Type 2 Diabetes. *J Diabetes Res*. 2020;2020:1682904.
- Jung IR, Ahima RS, Kim SF. Time-restricted feeding ameliorates MCDD-induced steatohepatitis in mice. *bioRxiv*. 2023.
- Tzeng TF, Tzeng YC, Cheng YJ, Liou SS, Liu IM. The ethanol extract from *Loniceria japonica* thunb. Regresses nonalcoholic steatohepatitis in a

- Methionine- and Choline-Deficient Diet-Fed animal model. *Nutrients*. 2015;7(10):8670–84.
25. Wang Q, Wei Y, Wang Y, Yu Z, Qin H, Zhao L, Cheng J, Shen B, Jin M, Feng H. Total flavonoids of *broussonetia papyrifera* alleviate non-alcohol fatty liver disease via regulating Nrf2/AMPK/mTOR signaling pathways. *Biochim Biophys Acta Mol Cell Biol Lipids*. 2024;1869(5):159497.
26. Chen YJ, Song HY, Zhang ZW, Chen Q, Tang ZP, Gu M. Extracts of vine tea improve Diet-Induced Non-Alcoholic steatohepatitis through AMPK-LXRα signaling. *Front Pharmacol*. 2021;12:711763.
27. Hu J, Zheng Y, Ying H, Ma H, Li L, Zhao Y. Alanyl-Glutamine Protects Mice against Methionine- and Choline-Deficient-Diet-Induced Steatohepatitis and Fibrosis by Modulating Oxidative Stress and Inflammation. *Nutrients*. 2022;14(18).
28. Di Ciaula A, Calamita G, Shanmugam H, Khalil M, Bonfrate L, Wang DQ, Baffy G, Portincasa P. Mitochondria matter: systemic aspects of nonalcoholic fatty liver disease (NAFLD) and diagnostic assessment of liver function by stable isotope dynamic breath tests. *Int J Mol Sci*. 2021;22(14).
29. Vesković M, Labudović-Borović M, Mladenović D, Jadžić J, Jorgačević B, Vukićević D, Vučević D, Radosavljević T. Effect of betaine supplementation on liver tissue and ultrastructural changes in Methionine-Choline-Deficient Diet-Induced NAFLD. *Microsc Microanal*. 2020;26(5):997–1006.
30. Xiao J, Wang F, Liong EC, So KF, Tipoe GL. Lycium barbarum polysaccharides improve hepatic injury through NFκB and NLRP3/6 pathways in a methionine choline deficient diet steatohepatitis mouse model. *Int J Biol Macromol*. 2018;120(Pt B):1480–9.
31. Yu CJ, Wang QS, Wu MM, Song BL, Liang C, Lou J, Tang LL, Yu XD, Niu N, Yang X, et al. TRUSS exacerbates NAFLD development by promoting IkBα degradation in mice. *Hepatology*. 2018;68(5):1769–85.
32. Seedorf K, Weber C, Vinson C, Berger S, Vuillard L-M, Kiss A, Creusot S, Broux O, Geant A, Ilic C. Selective disruption of Nrf2-KEAP1 interaction leads to NASH resolution and reduction of liver fibrosis in mice. *Jhep Rep*. 2023;5(4):100651.
33. Zhu L, Wang N, Guo G, Fan Z, Shi X, Ji X. Male zooid extracts of *antheraea pernyi* ameliorates non-alcoholic fatty liver disease and intestinal dysbacteriosis in mice induced by a high-fat diet. *Front Cell Infect Microbiol*. 2022;12:1059647.
34. Zhao CZ, Jiang W, Zhu YY, Wang CZ, Zhong WH, Wu G, Chen J, Zhu MN, Wu QL, Du XL, et al. Highland barley *monascus purpureus* extract ameliorates high-fat, high-fructose, high-cholesterol diet induced nonalcoholic fatty liver disease by regulating lipid metabolism in golden hamsters. *J Ethnopharmacol*. 2022;286:114922.
35. Schlaepfer IR, Joshi M. CPT1A-mediated fat oxidation, mechanisms, and therapeutic potential. *Endocrinology*. 2020;161(2).
36. Du T, Xiang L, Zhang J, Yang C, Zhao W, Li J, Zhou Y, Ma L. Vitamin D improves hepatic steatosis in NAFLD via regulation of fatty acid uptake and β-oxidation. *Front Endocrinol (Lausanne)*. 2023;14:1138078.
37. Lee J, Choi J, Selen Alpergin ES, Zhao L, Hartung T, Scafi S, Riddle RC, Wolfgang MJ. Loss of hepatic mitochondrial Long-Chain fatty acid oxidation confers resistance to Diet-Induced obesity and glucose intolerance. *Cell Rep*. 2017;20(3):655–67.
38. Li J, Qi J, Tang Y, Liu H, Zhou K, Dai Z, Yuan L, Sun C. A nanodrug system overexpressed CircRNA_0001805 alleviates nonalcoholic fatty liver disease via miR-106a-5p/miR-320a and ABCA1/CPT1 axis. *J Nanobiotechnol*. 2021;19(1):363.
39. He A, Chen X, Tan M, Chen Y, Lu D, Zhang X, Dean JM, Razani B, Lodhi IJ. Acetyl-CoA derived from hepatic peroxisomal β-Oxidation inhibits autophagy and promotes steatosis via mTORC1 activation. *Mol Cell*. 2020;79(1):30–e4234.
40. Schneider KM, Mohs A, Kilic K, Candels LS, Elfers C, Bennek E, Schneider LB, Heymann F, Gassler N, Penders J, et al. Intestinal microbiota protects against MCD Diet-Induced steatohepatitis. *Int J Mol Sci*. 2019;20(2):308.
41. Vahid F, Rahmani D, Davoodi SH. The correlation between serum inflammatory, antioxidant, glucose handling biomarkers, and dietary antioxidant index (DAI) and the role of DAI in obesity/overweight causation: population-based case-control study. *Int J Obes (Lond)*. 2021;45(12):2591–9.
42. Somme E, Montandon SA, Loizides-Mangold U, Gaia N, Lazarevic V, De Vito C, Perroud E, Bochaton-Piallat ML, Dibner C, Schrenzel J, et al. The GLP-1R agonist liraglutide limits hepatic lipotoxicity and inflammatory response in mice fed a methionine-choline deficient diet. *Transl Res*. 2021;227:75–88.
43. Wang Q, Ou Y, Hu G, Wen C, Yue S, Chen C, Xu L, Xie J, Dai H, Xiao H, et al. Naringenin attenuates non-alcoholic fatty liver disease by down-regulating the NLRP3/NF-κB pathway in mice. *Br J Pharmacol*. 2020;177(8):1806–21.
44. Kaur J, Kumar V, Kumar V, Shafi S, Khare P, Mahajan N, Bhadada SK, Kondepudi KK, Bhunia RK, Kuhad A, et al. Combination of TRP channel dietary agonists induces energy expending and glucose utilizing phenotype in HFD-fed mice. *Int J Obes (Lond)*. 2022;46(1):153–61.
45. Parlati L, Régnier M, Guillou H, Postic C. New targets for NAFLD. *Jhep Rep*. 2021;3(6):100346.
46. Yao Z, Zhou H, Figeys D, Wang Y, Sundaram M. Microsome-associated luminal lipid droplets in the regulation of lipoprotein secretion. *Curr Opin Lipidol*. 2013;24(2):160–70.
47. Zeng H, Qin H, Liao M, Zheng E, Luo X, Xiao A, Li Y, Chen L, Wei L, Zhao L, et al. CD36 promotes de Novo lipogenesis in hepatocytes through INSIG2-dependent SREBP1 processing. *Mol Metab*. 2022;57:101428.
48. Lian CY, Zhai ZZ, Li ZF, Wang L. High fat diet-triggered non-alcoholic fatty liver disease: A review of proposed mechanisms. *Chem Biol Interact*. 2020;330:109199.
49. Lee E, Korf H, Vidal-Puig A. An adipocentric perspective on the development and progression of non-alcoholic fatty liver disease. *J Hepatol*. 2023;78(5):1048–62.
50. Wu X, Xu N, Li M, Huang Q, Wu J, Gan Y, Chen L, Luo H, Li Y, Huang X, et al. Protective effect of Patchouli alcohol against High-Fat diet induced hepatic steatosis by alleviating Endoplasmic reticulum stress and regulating VLDL metabolism in rats. *Front Pharmacol*. 2019;10:1134.
51. Sheng D, Zhao S, Gao L, Zheng H, Liu W, Hou J, Jin Y, Ye F, Zhao Q, Li R, et al. BabaoDan attenuates high-fat diet-induced non-alcoholic fatty liver disease via activation of AMPK signaling. *Cell Biosci*. 2019;9:77.
52. Serrano-Maciá M, Simón J, González-Rellán MJ, Azkargorta M, Goikoetxea-Usandizaga N, Lopitz-Otsoa F, De Urturi DS, Rodríguez-Agudo R, Lachiondo-Ortega S, Mercado-Gomez M, et al. Neddylation Inhibition ameliorates steatosis in NAFLD by boosting hepatic fatty acid oxidation via the DEPTOR-mTOR axis. *Mol Metab*. 2021;53:101275.

Publisher's Note

Springer Nature remains neutral with regard to jurisdictional claims in published maps and institutional affiliations.